tvst

Neuro-Ophthalmology

Description of a Nonhuman Primate Model of Retinal Ischemia/Reperfusion Injury

Li Gong[1], Louis R. Pasquale[2], Janey L. Wiggs[3], Lingzhen Pan[1], Zhenyan Yang[1], Mingling Wu[1], Zirui Zeng[1], Zunyuan Yang[1], Yubo Shen[1], Dong Feng Chen[4], and Wen Zeng[1]

[1] PriMed Non-human Primate Research Center of Sichuan PriMed Shines Bio-tech Co., Ltd., Ya'an, Sichuan Province, China
[2] Eye and Vision Research Institute at New York Eye and Ear Infirmary of Mount Sinai, Icahn School of Medicine at Mount Sinai, New York, NY, USA
[3] Massachusetts Eye and Ear, Department of Ophthalmology, Harvard Medical School, Boston, MA, USA
[4] Schepens Eye Research Institute of Massachusetts Eye and Ear, Department of Ophthalmology, Harvard Medical School, Boston, MA, USA

Correspondence: Wen Zeng, PriMed Non-Human Primate Research Center of Sichuan PriMed Shines Bio-tech Co., Ltd., Ya'an, Sichuan Province 625000, China.
e-mail: zengwen@scprimed.com
Dong Feng Chen, Schepens Eye Research Institute of Massachusetts Eye and Ear, Department of Ophthalmology, Harvard Medical School, Boston, MA 02114, USA.
e-mail: dongfeng_chen@meei.harvard.edu

Received: March 25, 2023
Accepted: May 29, 2023
Published: June 22, 2023

Keywords: retinal ischemia-reperfusion injury; nonhuman primate; animal model

Citation: Gong L, Pasquale LR, Wiggs JL, Pan L, Yang Z, Wu M, Zeng Z, Yang Z, Shen Y, Chen DF, Zeng W. Description of a nonhuman primate model of retinal ischemia/reperfusion injury. Transl Vis Sci Technol. 2023;12(6):14, https://doi.org/10.1167/tvst.12.6.14

Purpose: To establish an inducible model of retinal ischemia/reperfusion injury (RI/RI) in nonhuman primates (NHPs) to improve our understanding of the disease conditions and evaluate treatment interventions in humans.

Methods: We cannulated the right eye of rhesus macaques with a needle attached to a normal saline solution reservoir at up to 1.9 m above the eye level that resulted in high intraocular pressure of over 100 mm Hg for 90 minutes. Retinal morphology and function were monitored before and after RI/RI over two months by fundus photography, optical coherence tomography, electroretinography, and visual evoked potential. Terminal experiments involved immunostaining for retinal ganglion cell marker Brn3a, glial fibrillary acidic protein, and quantitative polymerase chain reaction to assess retinal inflammatory biomarkers.

Results: We observed significant and progressive declines in retinal and retinal nerve fiber layer thickness in the affected eye after RI/RI. We noted significant reductions in amplitudes of electroretinography a-wave, b-wave, and visual evoked potential N2-P2, with minimal recovery at 63 days after injury. Terminal experiments conducted two months after injury revealed ~73% loss of retinal ganglion cells and a fivefold increase in glial fibrillary acid protein immunofluorescence intensity compared to the uninjured eyes. We observed marked increases in tumor necrosis factor–alpha, interferon-gamma, interleukin-1beta, and inducible nitric oxide synthase in the injured retinas.

Conclusions: The results demonstrated that the pathophysiology observed in the NHP model of RI/RI is comparable to that of human diseases and suggest that the NHP model may serve as a valuable tool for translating interventions into viable treatment approaches.

Translational Relevance: The model serves as a useful platform to study potential interventions and treatments for RI/RI or blinding retinal diseases.

Introduction

Retinal ischemia/reperfusion injury (RI/RI) occurs in various retinal diseases, including diabetic retinopathy, glaucoma, and vascular ischemic retinopathy.[1] RI/RI, which results in permanent loss of retinal ganglion cells (RGCs), is a common cause of severe vision impairment and blindness in middle-aged and elderly patients.[2] Currently, no effective treatment is available for RI/RI, and the underlying mechanisms of reperfusion-induced retinal neuron injury are not fully understood.[3] The lack of adequate treatments for RI/RI may be due to the limited availability of a viable

model that would translate such treatments to human disease.

Much effort is focused on strategies to rescue structure and function during RI/RI in murine models where the macula is absent and retinal vessels have a spoke-and-wheel architecture.[4] Although murine models provide the benefit of wide availability and ease of manipulation, there are differences in ocular anatomical, physiological, and immunological characteristics versus human eyes.[5] Thus the results obtained from these models may not always reflect human pathogenesis. Because the eyes of nonhuman primates (NHPs) most closely resemble the human eye, Gao et al.[6] developed a retinal artery I/R model based on injecting an autologous clot directly into the ophthalmic artery, and Choi et al.[7] investigated the macular vulnerability to ischemia in rhesus monkeys induced by incremental increases of intraocular pressure (IOP) to 70 mm Hg. Currently, there are no NHP models of global RI/RI, such as that induced by high IOP, showing fundus changes similar to humans.

Given the high prevalence of retinal ischemic disease from the collective effects of conditions like central retinal artery occlusion, acute glaucoma, and diabetic retinopathy, we developed an NHP model of RI/RI through acute IOP elevation for the subsequent use in pharmacokinetic and pharmacodynamics intervention studies. Here, we report that the monkeys developed RI/RI like those observed in human patients. The monkeys demonstrated structural and functional optic nerve and total retinal degeneration as well as upregulation of inflammatory biomarkers in the retina over two months.

Methods

Animals

We used 12 rhesus macaque monkeys (*Macaca mulatta,* ages 3–6 years) accommodated in the PriMed Non-human Primate Research Center (Ya'an, China) in this study. All monkeys were pair-housed in accordance with standard operating procedures of PriMed in a climate-controlled room at 18°C to 26°C with a relative humidity of 40% to 70%, a 12-hour light/12-hour dark cycle, and a ventilation rate of eight times/hour. Monkeys had free access to drinking water and were continually fed with monkey chow (4% calories from fat, 16% calories from protein, and 80% calories from carbohydrates) at 200 to 300 g/d. We also provided a daily allotment of fruits, vegetables, or additional supplements and various toys. This study complied with the National Institutes of Health Guide for the Care and Use of Laboratory Animals and the Association for Research of Vision and Ophthalmology guidelines. The Institutional Animal Care and Use Committee of PriMed Non-Human Primate Research Center of Sichuan Primed Shines Bio-tech Co., Ltd, reviewed and approved the experimental protocols.

RI/RI

Monkeys were anesthetized with intramuscular injection of ketamine (8 mg/kg) and xylazine (8 mg/kg). Heart rate and arterial oxyhemoglobin saturation were monitored continuously (prince-100; Heal Force Inc., Shanghai, China) and maintained above 75 beats/min and 95%, respectively. We induced retinal ischemia (RI) in the right eye, with the fellow eye of the same monkey serving as a control. The anterior chamber was cannulated by the insertion of a 30-gauge needle into the peripheral cornea. The needle was connected via polyethylene tubing (Kangning Inc., Sichuan, China) to an adjustable-height reservoir of sterile normal saline solution (Kelun Pharmaceutical Co., Ltd., Sichuan, China) (Fig. 1). Acute IOP elevation was induced unilaterally in nine monkeys (four females and five males) by cannulating the anterior chamber with a saline reservoir bag at 190 cm above eye level for 90 minutes. After anterior chamber cannulation, we observed rapid onset conjunctival and iris blood vessel blanching, corneal edema, and retinal pallor. Preliminarily, we cannulated the anterior chambers of 3 other male monkeys with a saline reservoir bag at 170 cm above the eye level for 90 minutes. IOP was measured by a handheld tonometer (TA01i, Helsinki, Finland) in monkey eyes, and pressure in the eye was elevated by adjusting the distance every five minutes, to 130 cm, 150 cm, and 170 cm above the eye level (Table 1). After IOP reached its targeted values for 90 minutes, the saline reservoir was slowly lowered, and the needle was withdrawn from the eye. The disappearance and subsequent reappearance of vessels in the fundus on fluorescein angiography served to document ischemia-reperfusion of the retina.

Fundus Photography and Optical Coherence Tomography

We performed fundus photography (FP) and optical coherence tomography (OCT) for both eyes of each monkey to evaluate changes in the thickness of the retinal layers including the retinal nerve fiber layer (RNFL), inner nuclear layer (INL), outer nuclear layer (ONL) and the average total retinal thickness after RI/RI (Fig. 1). Monkeys were anesthetized, and the

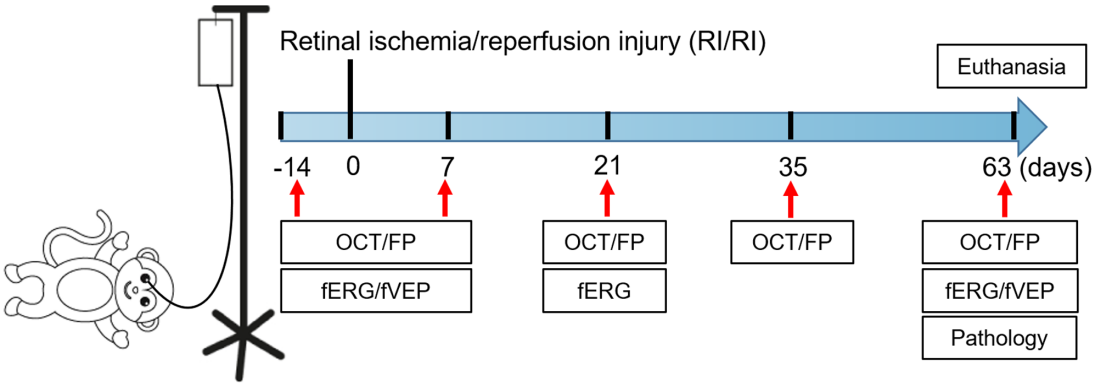

Figure 1. Schematic illustration of the RI/RI model and experimental schedules.

Table 1. Records of Retinal Ischemia/Reperfusion Injury Induction in One NHP

Start Time	Height of Reservoir (cm)	Corresponding Hydrostatic Pressure (mm Hg)	IOP Measured by Tonometer (mm Hg)	Cornea	Fundus Fluorescein Angiography
9:30	100	74	62	Normal	—
9:35	130	96	82	Normal	—
9:40	150	110	88	Normal	—
9:45	170	125	>100	Mild Edema	09:45–09:52

pupil was dilated as previously described.[8] Monkeys were placed in a dark room until the pupil diameter reached ≥6 mm measured with a caliper. After positioning the monkeys in a headrest, we placed a self-retaining eyelid speculum to enable the examination. Macula-centered images were obtained using a Kowa retinal camera (VX-20, Tokyo, Japan).

After FP, an evenly illuminated, well-focused fundus image with high-quality OCT images was acquired using the Heidelberg Spectralis OCT Plus (Heidelberg Engineering GmbH, Heidelberg, Germany) as previously described.[8] All OCT images had quality scores ≥25. The images of optic nerve head scans were obtained by circular scans centered on the optic disc at a 3.4 mm diameter circle. The Heidelberg OCT built-in software automatically segmented and measured the circumpapillary RNFL thickness in six sectors. The means of the sectoral RNFL thicknesses were calculated to determine the global RNFL thickness. Macula-centered OCTs were obtained with the fast macular scan procedure to measure the macula thickness. The built-in software of Heidelberg OCT generated a topographical map of the macula. The thickness of the total retina, INL and ONL from each of the nine Early Treatment of Diabetic Retinopathy Study subfields centered on the fovea were collected in each subject and averaged.

Full-Field Electroretinography (ERG) and Visual-Evoked Potential (VEP)

ERG and VEP were performed to assess retinal and optic nerve conductive functions, respectively, after RI/RI (Fig. 1). ERG and VEP recordings were performed in a dark room under the dim red safety light. Monkeys were anesthetized, and the pupil was dilated as previously described. Stainless-steal needle electrodes were passed intracutaneously to a position 10 mm above the inion and directly over the vertex. The reference electrode was placed intracutaneously at the midpoint of the binoculus and the ground electrode was implanted into the tail. The VEP recordings were evaluated in terms of the amplitude of peaks P2 and N2. The amplitude was defined as the difference between N2 and P2 (A = N2 − P2). We performed ERG recordings immediately after collecting the VEP data. Recording gold lens electrodes were placed on both corneas. The reference electrodes were placed subcutaneously at the ipsilateral canthus, and the ground electrode was implanted at the midpoint of the binoculus. Electrode impedance was accepted when < 5 kΩ. We measured photopic ERG a-waves from the baseline to the cornea-negative peak, and we measured b-waves from the cornea-negative peak to the major cornea-positive peak. The ERG and VEP

recordings were performed following the guidelines set by the International Society for Clinical Electrophysiology of Vision.[9] Data were processed by the software included in the ERG/VEP recorder (Ganzfeld Q450; Roland Consult Stasche & Finger GmbH, Brandenburg, Germany).

Retinal Ganglion Cell Counts and Immunohistochemistry

Three monkeys who underwent acute elevation of IOP after exposure to a 190 cm saline reservoir above the eye for 90 minutes were killed on day 63 after RI/RI. Eyes were enucleated, and the posterior poles with optic nerve head and macula (approximately 0.8 cm × 1.6 cm) were dissected and fixed in formaldehyde–acetic acid–ethanol fixative (15:10:60 v/v) for 72 hours before being embedded in paraffin. The remaining retinas were stored at −80°C for quantitative polymerase chain reaction (qPCR).

One hundred slices at 5 µm/section were cut at the fovea, and slices were collected on silane-coated slides for immunostaining. Eight slices were immunolabeled for astrocyte marker, glial fibrillary acid protein (GFAP),[10] and the other eight slices were stained for RGC marker, Brn-3a.[11] Before immunostaining, slides were deparaffinized and rehydrated. Slides were soaked in ethylenediamine tetra-acetic acid under a hot water bath for antigen retrieval. A 3% H_2O_2 solution was used to remove endogenous peroxidase. Nonspecific binding sites were blocked by incubation with goat serum containing 5% bovine serum albumin for 20 minutes at room temperature. Slides were incubated with a primary antibody against GFAP (Abcam, Cambridge, UK) or Brn-3a (Merck-Millipore, Darmstadt, Germany) at 37°C overnight. A secondary antibody (SP-9000; ZSGB-BIO, Beijing, China) was added and incubated for 20 minutes at room temperature. Horseradish peroxidase–streptavidin working solution was added and kept at 37°C for 20 minutes. The bound antibody-peroxidase complexes on the sections were visualized using a 3,3-diaminobenzidine tetrahydrochloride substrate solution consisting of 1.5 mg 3,3-diaminobenzidine tetrahydrochloride and 50 µL 30% hydrogen peroxide, in 10 mL 0.1 M Tris, pH 7.6. The sections were incubated in the dark until brown staining appeared, washed in distilled water, counterstained with hematoxylin, dehydrated, and placed under a coverslip with Permount (Solarbio, Beijing, China). Control sections were treated similarly except we omitted the primary antibody. The integrated optical density of GFAP staining was measured by imaging analysis software (Image-Pro Plus 6.0; Media Cybernetics, Inc., Rockville, MD, USA). The 1.5 mm regions at the nasal and temporal sides of the fovea were photographed at magnification ×200 with a microscope (Olympus BX43F; Olympus, Tokyo, Japan). The numbers of RGCs stained with Brn-3a were counted. The percentage of RGC loss was determined by dividing the RGC number obtained from the retina with ischemic injury by that of the contralateral control retina of the same monkey. Two investigators conducted all quantification procedures in a masked fashion.

Real-Time Quantitative PCR To Detect Cytokine Expression in the Retinas

Total RNA was extracted from the retinas using RNAeasy Plus Kit (Qiagen, Hilden, Germany) according to the manufacturer's protocol. The Superscript III First Strand Kit (Invitrogen, Carlsbad, CA, USA) was used to synthesize cDNA from total RNA. The qPCR reaction was carried out in a 20 µL system containing 0.8 µL of specific primers (10 µM), 10 µL of 2 × Master Mix from a KAPA SYBR Fast qPCR kit (Kapa Biosystems Inc., Wilmington, DE, USA), 2.0 µL of template DNA, and 7.2 µL of double-distilled water. Quantitative detection of specific mRNA transcripts were performed by real-time PCR using the real-time PCR system (Eppendorf, Westbury, NY, USA). The sequences of primers of tumor necrosis factor–alpha (TNF-α), interferon-gamma (IFN-γ), interleukin-1 beta (IL-1β), and inducible nitric oxide synthase (iNOS) are listed in Table 2. Relative amounts of

Table 2. List of Primer Sequences Used in Real-Time PCR

Gene	Forward	Reverse
β-Actin	TCGTGCGTGACATTAAGGAGAAGC	TCGTTGCCAATGGTGATGACCTG
TNF-α	AATGGCGTGGAGCTGACAGATAAC	CGATGCGGCTGATGGTGTGG
IFN-γ	CGAATGTCCAACGCAAAGCAGTAC	TGCTCTTCGACCTCGAAACATCTG
IL-1β	CTTACTACAGCGGCAACGAGGATG	CCACCACCCAGAGGGCAGAG
iNOS	TCACAGCCTCAGCAAGCAGCAGAATG	GCCTTGTGGTGAAGTGTGTCCTGGAA

specific mRNA transcript were presented in fold changes by normalization to the expression level of the β-Actin housekeeping gene.

Statistical Analysis

We used GraphPad Prism 8.0 software (GraphPad Software Inc., La Jolla, CA, USA) to perform all statistical analyses. The performed tests were two-sided, and $P < 0.05$ was considered statistically significant. Unpaired *t*-tests were performed to assess differences in injured versus uninjured eyes, whereas paired *t*-tests were used to compare eyes in follow-up from baseline.

Results

IOP Elevation and Retinal Ischemia

To establish an NHP model of global RI/RI using the approach of acute elevation IOP, we began by defining the level of IOP required for inducing retinal ischemia. The existing models of retinal ischemia by elevated IOP up to 100 mm Hg did not show sustained structural and functional changes like humans.[12] Thus we initiated pilot studies by increasing IOP to 100 mm Hg and higher. When the saline reservoir was elevated to 170 cm or above eye level, corneal edema was observed within a few minutes after IOP elevation. The normal retina (Fig. 2A) became opaque, the optic disc margins were obscured, and the retinal vessels were narrowed in caliber (Fig. 2B). After the needle was withdrawn from the anterior chamber, the optic disc margins were sharp, and the caliber of the arterioles increased compared to the baseline (Fig. 2C).

After intravenous fluorescein injection, dye passed through the short posterior ciliary arteries and appeared in the optic nerve and choroid within 12 seconds (Figs. 2D–F) in normal eyes. After the saline reservoir was elevated to 170 cm, delays in the filling of cilioretinal arteries and corneal edema were evident in retinal ischemia-treated eyes (Figs. 2G–O) compared to the normal eye (Figs. 2D–F) and RI-treated eye after reperfusion (Figs. 2M–O). However, no obvious change was found in the retina, the retinal vessels, RNFL thickness, or global retinal thickness up to 63 days after 90 minutes of raising the saline reservoir to 170 cm (Supplementary Fig. S1).

In subsequent experiments, we increased the IOP by raising the reservoir to 190 cm above eye level for 90 minutes. Presumed IOPs were likely above 100 mm Hg but could not be measured accurately.

Progressive Thinning of RNFL After RI/RI

Fundus photos displayed retinal and optic disc swelling due to ischemia at seven days after RI/RI of 190 cm for 90 minutes. At day 63 after RI/RI, optic disc pallor, and thinning of the retinal arterioles were noted (Figs. 3A–C). An insignificant mean global RNFL thickness increase was noted at day 7 after RI/RI (12 $\pm$ 20 µm OD vs. 1 $\pm$ 1 µm OS; $P = 0.13$) (Fig. 3J), which was marked by significant hyper-reflectivity and swelling on structural OCT (Figs. 3D, 3E). Significant declines started at day 21 in injured eyes ($P < 0.001$ vs. OS) (Figs. 3F, 3J). Total retinal thickness decreased from seven days after RI/RI compared to baseline (-44 ± 27 µm OD vs. -1 ± 4 µm OS; $P = 0.004$), extending to day 63 (-84 ± 22 µm OD vs. -2 ± 3 µm OS; $P < .0001$) (Figs. 3G–I, 3L).

The INL thickness decreased from seven days after RI/RI compared to baseline (-15 ± 8 µm OD vs. 0 ± 1 µm OS; $P < 0.0001$), extending to day 63 (-19 ± 8 µm OD vs. 0 ± 1 µm OS; $P < 0.0001$) (Fig. 3O). The ONL thickness increased significantly at day 7 after RI/RI (6 ± 4 µm OD vs. 0 ± 1µm OS; $P = 0.001$) and showed no obvious change from day 21 to day 63 (Fig. 3Q). The uninjured contralateral eyes showed no RNFL swelling or retinal thickness change during the study (Figs. 3K, 3M, 3P, 3R).

RI/RI-Induced Loss of Retinal Function and Optic Nerve Conductivity

Acute retinal ischemic injury is reported to cause damage to the neuroretina, including photoreceptors and the RGC, whose function can be assessed through whole-field ERG and VEP.[13,14] To evaluate the functional effect of RI/RI, ERG and VEP measurements were performed after injury. RI/RI of 190 cm for 90 minutes produced significant declines in amplitudes of the light-adapted a-wave (7.9 ± 5.1 µv), b-wave (21.1 ± 12.5 µv), and VEP N2-P2 (17.0 ± 12.7 µv) compared to before induction (22.7 ± 4.6 µv, 63.4 ± 15.0 µv, and 39.9 ± 7.4 µv for the a-wave, b-wave, and VEP N2-P2, respectively; $P \leq 0.0024$) with minimal recovery by day 63 (10.3 ± 5.1 µv, 27.1 ± 13.8 µv and 22.0 ± 16.9 µv for the a-wave, b-wave, and VEP N2-P2, respectively; $P \leq 0.035$) (Fig. 4). In contrast, RI/RI by 170 cm of saline solution for 90 minutes and the uninjured contralateral eyes showed no change in a- and b- wave amplitudes (Supplementary Figs. S2, S3).

Quantification of RGC Loss and Retinal Immune Responses

Selected animals were killed for pathological examinations to determine the impacts of RI/RI on retinal

neuron survival and astrocytes and whether the acute ischemic injury in the retina induces a prolonged phase of neurodegeneration. RGC loss and GFAP intensity were quantified 63 days after ischemic injury (Fig. 5A). There was a 73% decline in total RGC counts (n = 3; $P = 0.0034$ vs. OS) (Fig. 5B) and a fivefold astrocytic activation versus the uninjured eyes (n = 3; $P = 0.007$) (Fig. 5C). Upregulation of GFAP is a hallmark of reactive astrocytes and commonly used to assess their responses. RI/RI led to a significant increase in GFAP expression in the retinas and RGC degeneration two months after the initial insult.

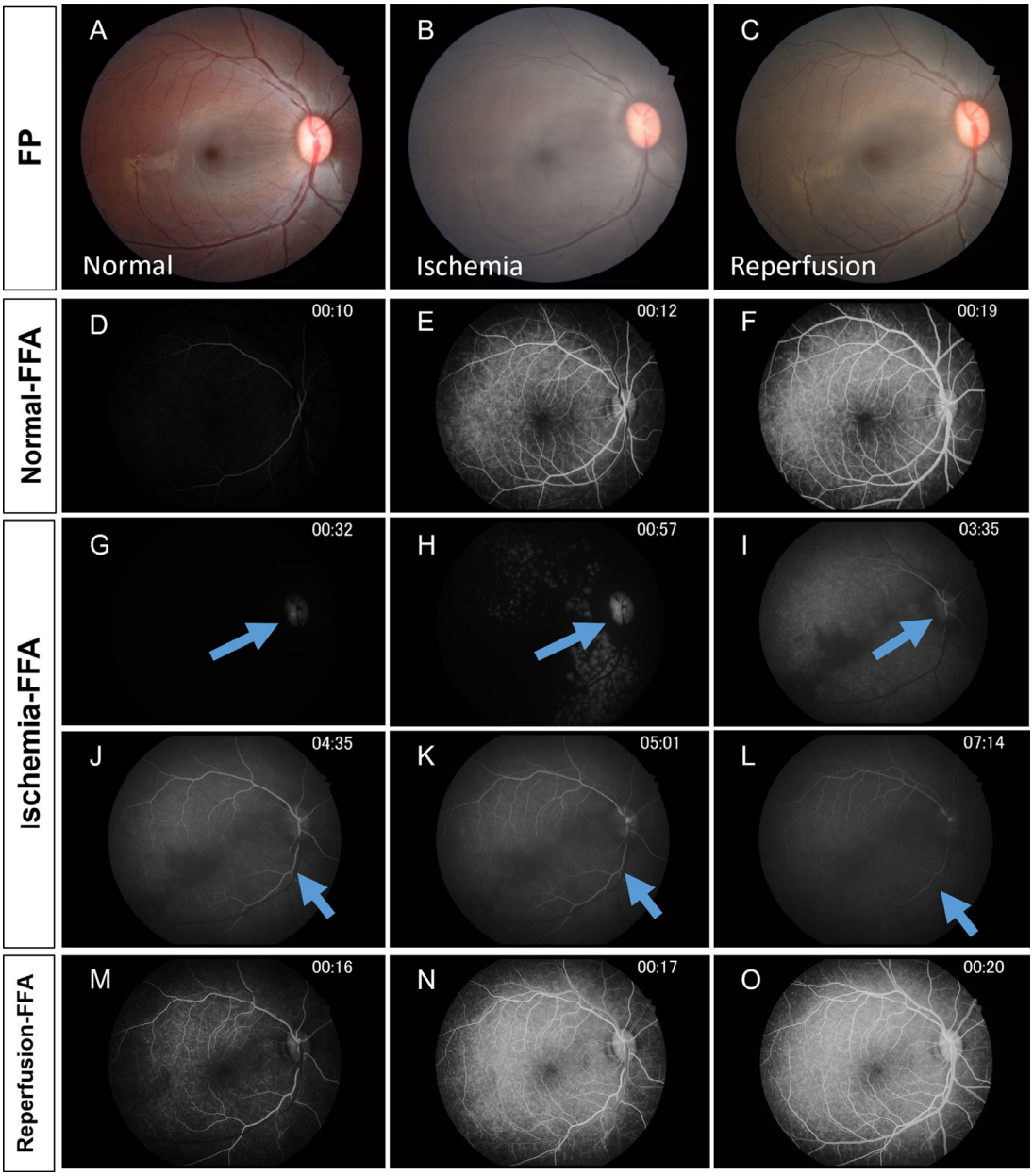

Figure 2. Retinal and choroidal perfusion in a normal and in retinal ischemia (170 cm saline solution) monkey. Fundus photographs (FPs) before (**A**) and at seven minutes after anterior chamber cannulation to 170 cm above the eye level (**B**). Note that in the retina ischemia (RI)–treated eye, the retina became opaque, optic disc margins were obscured, and the caliber of the retinal arterioles was markedly attenuated, especially near the optic disc. (**C**) An FP during reperfusion after the needle was withdrawn from the anterior chamber. The optic disc margins were sharp, and the caliber of the arterioles increased compared to the baseline. Fundus fluorescein angiograms (FFA) of retinal ischemia (**G**–**L**) and during reperfusion (**M**–**O**) eyes show filling of retinal and choroidal vessels at different time points (inset) after injection. Note the filling of cilioretinal arteries (*blue arrows*) in the RI-treated eye showed delays (**G**–**L**) compared to the normal eye (**D**–**F**) and RI-treated eye after reperfusion (**M**–**O**).

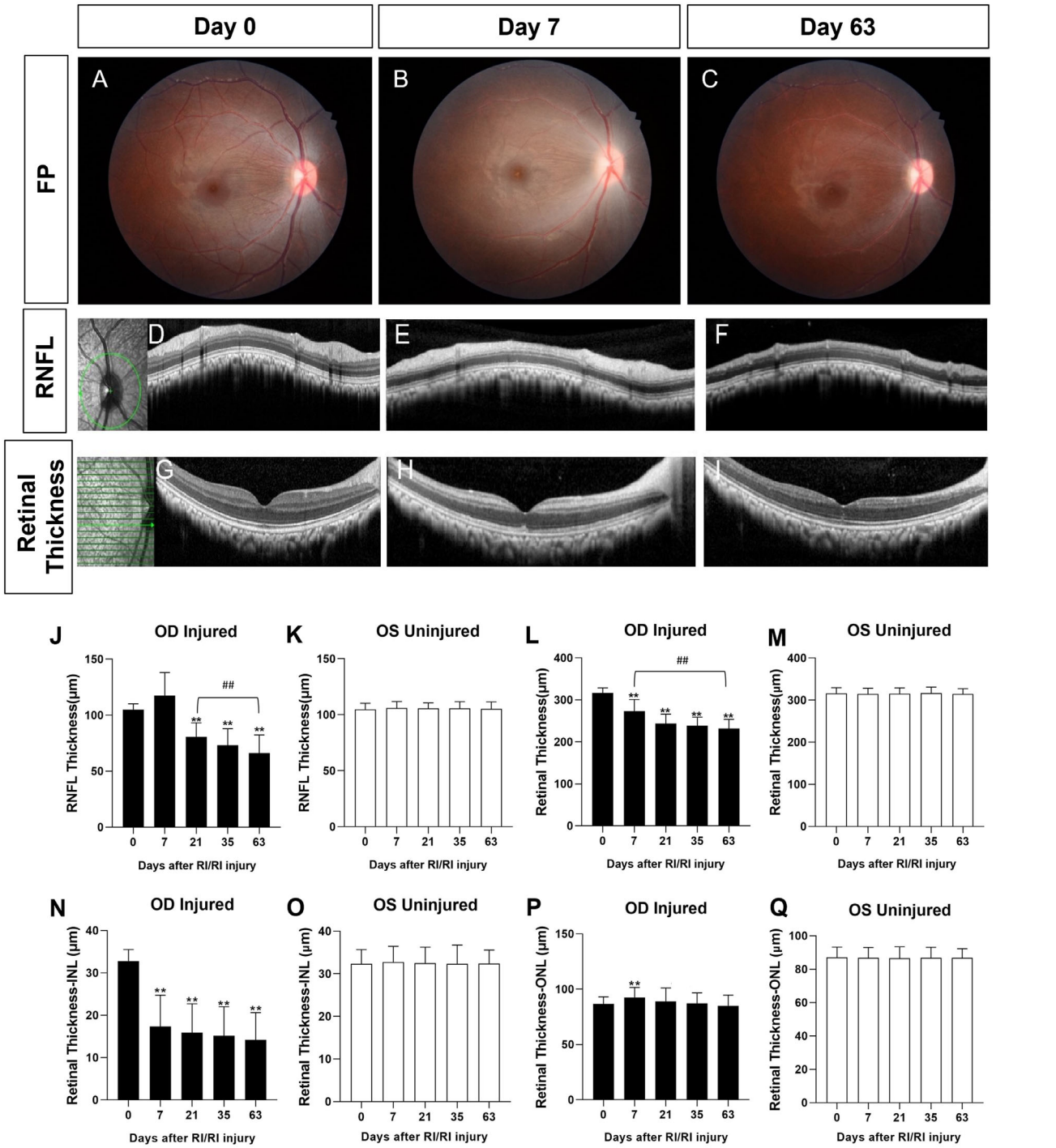

Figure 3. Progressive degeneration of retina after RI/RI. (**A**–**C**) Fundus photographs taken at days 0, 7, and 63 post-RI/RI. Note the optic disc pallor and thinning of the retinal arterioles at day 63 post-RI/RI. Circumpapillary (**D**–**F**) and macula-region (**G**–**I**) OCT depicting the RNFL and retinal thickness at days 0, 7, and 63 after RI/RI. Note the hyper-reflectivity and swelling of RNFL at day 7 and thinning of the RNFL and global retina at day 63. (**J**–**M**) Quantification of global RNFL (**J**, **K**), retinal (**L**, **M**), INL (**N**, **O**) and ONL (**P**, **Q**) thickness in RI (*black bars*) and contralateral control eyes (*white bars*) (n = 9). Note an insignificant global RNFL thickness increase and a significant ONL thickness increase at day 7 after RI/RI and significant declines of global RNFL thickness started at day 21 in injured eyes, extending to day 63. Total retinal thickness and INL thickness decreased from seven days after RI/RI compared to baseline, extending to day 63. $^{**}P < 0.01$ versus day 0 by paired *t*-test; $\#\#P < 0.01$ versus different timepoints by paired *t*-test.

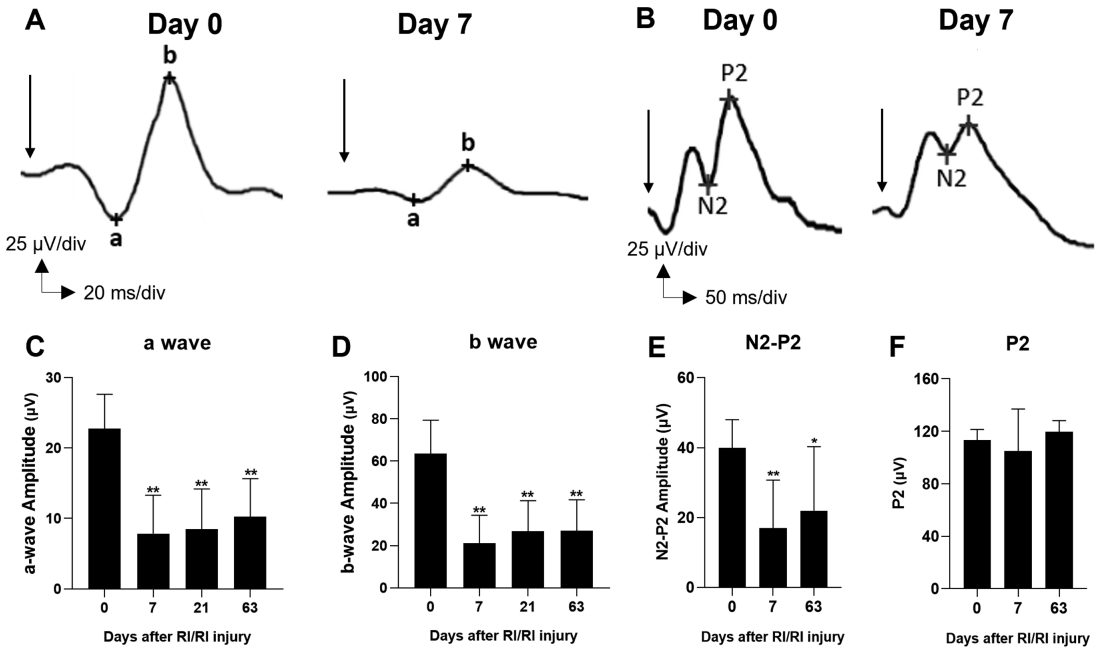

Figure 4. Change of retinal and optic nerve function after RI/RI. (**A**, **B**) Representative waveforms of ERG a-wave and b-wave and VEP on days 0 and 7 post-RI/RI. C-F: Quantification of ERG a-wave (**C**) and b-wave (**D**) and VEP N2-P2 (**E**) and P2 (**F**) amplitudes. Note the significant reduction of ERG a-wave and b-wave and VEP N2-P2 amplitudes from day 0 to 7 that stayed low until day 63 after RI/RI (n = 7/group). *, $P < 0.05$; **, $P < 0.01$ vs. Day 0.

The effects of RI/RI on the expression of inflammatory cytokines were verified by qPCR. Marked increases in TNF-α (26.4-fold), IFN-γ (40-fold), IL-1β (10.5-fold), and iNOS (40-fold) ($P < 0.046$ vs. OS, three injured vs. six uninjured eyes) were noted (Fig. 6). Although the ischemic injury lasted for only 90 minutes, in the absence of any sustained injury, high levels of inflammatory cytokines and an enzyme responsible for the generation of free radicals (iNOS) remained present 63 days after RI/RI.

Discussion

Ischemia contributes to multiple conditions, including stroke,[15] acute coronary syndrome,[16] glaucoma,[17] diabetic retinopathy,[18] and central retinal artery occlusion.[19,20] Acute retinal ischemia caused by high IOP followed by reperfusion leads to neuronal and vascular degeneration[21] and is a stroke-equivalent that most commonly causes irreversible vision loss in the elderly.[17] It induces damage to the inner retina and permanent RGC loss.[22,23] Currently, no effective treatment is available for acute retinal ischemia, and the underlying mechanisms of reperfusion-induced retinal neuron injury are not fully understood. Here, we document for the first time, an NHP model of RI/RI with a prolonged phase of retinal degeneration that was sustained two months after the induction. Our findings suggest that continuous treatment may be needed after the acute phase of retinal ischemia because progressive thinning of the RNFL, INL, and total retina continued for two months after injury.

Investigators have used rodent and rabbit RI/RI models to study the mechanisms involved in retinal degeneration and to seek therapeutic approaches to prevent this degeneration.[23] Although murine and rabbit models are useful to study the underlying pathophysiology of retinal ischemia, distinctions in anatomical and physiological features between rodents and humans have limited translational potential of putative treatments. The results obtained from these models may not always reflect human pathogenesis.[24] The NHP models of RI would be useful to understand how ischemia affects the optic nerve and retinal neurons. Occlusion of the retinal artery alone by a clamp or autologous clot injection arrests retinal blood flow temporarily[6]; however, these models simulate acute retinal artery ischemia but do not reflect the pathogenesis of ischemia-induced diabetic retinopathy or acute glaucoma with high IOP, which usually can produce global retinal ischemia. IOP elevation through serial lasering to the trabecular meshwork has been used to induce the experimental glaucoma model in NHPs.[25] Such a technique induces chronic IOP eleva-

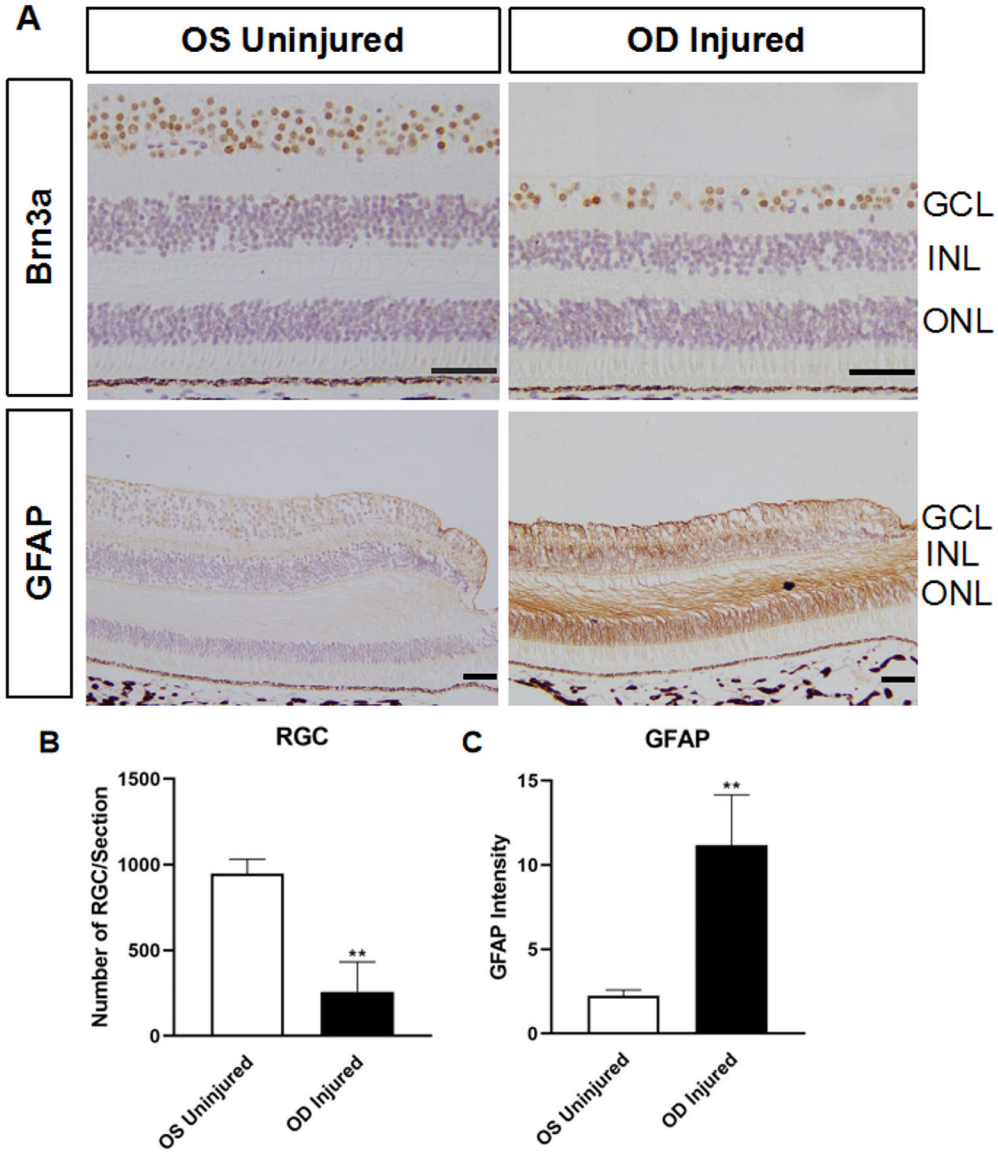

Figure 5. Loss of RGCs and induction of astroglial response in the retinas after RI/RI by 190 cm of saline solution for 90 minutes. (**A**) Photomicrographs of retinal sections taken from RI/RI-treated and contralateral eyes of rhesus monkeys at 63 days after injury that were immunolabeled for Brn3a and GFAP. (**B**) Quantification of Brn3a^{+} cells. (**C**) Quantification of GFAP intensity. $^{**}P < 0.01$ versus OS uninjured (n = 3/group). *Scale bars*: 100 µm (A).

tion but not reperfusion. Some scientists have reported RI/RI induced by elevating IOP in NHPs. Fortune et al.[25] measured peripapillary retinal thickness with a rapid rise in the IOP (to 45 mm Hg) in NHP. Choi et al.[7] observed responses of macular capillary vessel area density to elevations in IOP in NHP. They both reported that the changes in retinal thickness were minor. We also found IOP less than 100 mm Hg did not induce marked RGC loss and changes in retinal function. Cheung et al.[12] injected 100 µL of saline solution into the vitreous cavity of monkeys to achieve IOP levels above 100 mm Hg. The intervention disrupted blood flow in the fundus, but the longer-term damage to the retina was not examined. Furthermore, such a technique induces acute ischemia without reperfusion. In this study, we reported the structural and functional changes in the retina of a new RI/RI model in NHPs induced by elevating IOP higher than 100 mm Hg for 90 minutes.

Acute retinal edema and subsequent retinal atrophy in central retinal artery occlusion have been reported in animal models and clinically.[26] Cerebral edema can be secondary to disruption of the blood-brain barrier, local inflammation, vascular changes, or altered cellu-

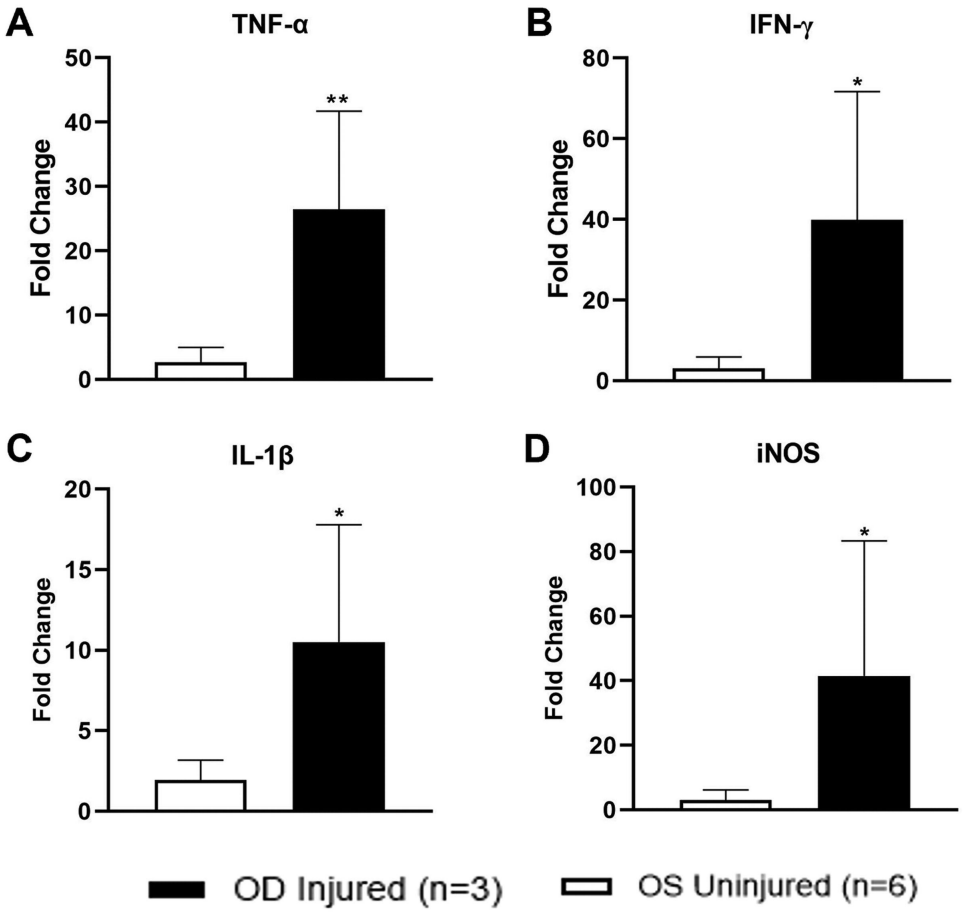

Figure 6. Induction of inflammatory cytokines in the retina after RI/RI. Marked increases in TNF-α (**A**), interferon-gamma (**B**), interleukin-1beta (**C**), and iNOS (**D**) in the RI-treated eyes compared to the contralateral control eye assessed by qPCR. $^{**}P < 0.01$ versus OS uninjured.

lar metabolism.[27] Reductions in selected regional brain volumes were found three months after clinical stroke.[28] In agreement with these findings in ischemic stroke of the brain, the RNFL thickness of our RI/RI models was found to increase seven days after RI/RI and decrease thereafter. Interestingly, disc swelling has also been reported in acute primary angle closure glaucoma.[29] It is suggested that retinal neuron loss in RI/RI and ischemic stroke injury share a common pathogenic process.

We observed a significant reduction of RGC counts and the whole retinal thickness two months after RI/RI. These results are consistent with the data from existing publications, which examined a few different points in time after ischemia.[22,30] Kim et al.[13] created IOP-induced retinal ischemia in a mouse model. RGC layer cell counts were significantly reduced starting from day 14. A significant thinning of the whole retinal thickness in ischemic eyes was measured beginning on day 21 after injury. VEP measures the conductivity of the RGCs and provides information about the function of the inner retinal and visual outcome.[31] In our study, the N2-P2 amplitude in VEP decreased significantly seven days after RI/RI and did not recover by two months, suggesting that persistent optic nerve injury occurs.

Several studies have reported that photoreceptors, amacrine cells, and bipolar cells are all sensitive to ischemic stress.[32–34] In our RI/RI model, INL and ONL thickness changed significantly after RI/RI. ERG a- and b-wave amplitudes are good indicators of the functional integrity of the photoreceptors and bipolar cells, respectively. Kim et al.[13] described a significant decrease of the a-wave amplitudes first at 21 days and 28 days after RI/RI that showed recovery at day 35. Our ERG data indicated that the a- and b-wave amplitudes decreased significantly from seven days to two months after induction without significant recovery. This variation could be due to the different compensatory responses to retinal ischemia between rodents and primates.

Recent investigations reveal that the eye elicits immunologic responses under pathophysiological stress. It was reported that ischemia-reperfusion injury

results in the sequestration of immune cells and inflammatory mediators to the ischemic region, which in turn induces local inflammatory responses.[1,35,36] In the absence of sustained insults, a prolonged phase of RGC degeneration exists after acute injury.[3] Astrocytes are active participants in the initiation and maintenance of post-ischemic inflammation. Retinal ischemia-reperfusion leads to astrocyte activation, proliferation, and the release of pro-inflammatory cytokines, chemokines, and reactive oxygen species.[3] In our RI/RI model, astrocyte activation still exists two months after RI/RI. The present study also revealed the expression of inflammatory cytokine increased two months after injury. In the absence of sustained insults, astrocyte activation and inflammation could be involved in propagating a prolonged phase of retinal degeneration after acute injury. The progressive structural loss of retina tissue over two months (Figs. 3J, 3L, 3O) suggests that there is an extended therapeutic window for saving vision in retinal ischemia.

There are ethical concerns regarding the use of NHP to study RI/RI. RI/RI was induced in one eye only to reduce excessive stress and the impact on behavior. We did not observe a functional visual loss in the monkeys we used in these experiments. It was necessary to use very high IOP to induce retinal ischemia, which resulted in obvious retinal degeneration. Another limitation of this study was only RGCs were counted immunohistologically and our study only lasted two months. Further studies on the effects of elevated IOP on photoreceptor and bipolar cell counts should be conducted to interpret the changes in ERG and retinal thickness.

To date, no effective treatment is available for acute retinal ischemia, and the existing animal models have limited efficacy in therapy development, although a timely intra-arterial tissue plasminogen activator injection for central retinal artery occlusion showed promise for improving vision in an uncontrolled clinical trial.[37] We successfully developed a new NHP model of RI/RI, which shows comparable clinical signs of sustained retinal degeneration. As an effective preclinical validation model, the NHP model may provide an opportunity to study the pathogenesis of RI/RI in more detail and facilitate the translation of interventions for humans.

Acknowledgments

Disclosure: **L. Gong**, PriMed (E, S); **L.R. Pasquale**, Twenty twenty (C), Nicox (C), Skye Biosciences (C), Character Bio (C), Eyenovia (C); **J.L. Wiggs**, Allergan (C), Editas(C), Maze (C),Regenxbio (C), Aerpio Pharmaceuticals (F); **L. Pan**, PriMed (E); **Z. Yang**, PriMed (E); **M. Wu**, PriMed (E); **Z. Zeng**, PriMed (E); **Z. Yang**, PriMed (E); **Y. Shen**, PriMed (E); **D.F. Chen**, Scientific Advisory Board of FireCyte Therapeutics, i-Lumen (C), PriMed (C), Biovisics Medical (C); **W. Zeng**, PriMed (E,S)

References

1. Minhas G, Sharma J, Khan N. Cellular stress response and immune signaling in retinal ischemia-reperfusion injury. *Front Immunol*. 2016;7:444.
2. Li Y, Hall NE, Pershing S, et al. Age, gender, and laterality of retinal vascular occlusion: a retrospective study from the IRIS Registry. *Ophthalmol Retina*. 2022;6:161–171.
3. Vu THK, Chen H, Pan L, et al. CD4^{+} T-cell responses mediate progressive neurodegeneration in experimental ischemic retinopathy. *Am J Pathol*. 2020;190:1723–1734.
4. Vestergaard N, Cehofski LJ, Honoré B, Aasbjerg K, Vorum H. Animal models used to simulate retinal artery occlusion: a comprehensive review. *Transl Vis Sci Technol*. 2019;8(4):23.
5. Samuels BC, Siegwart JT, Zhan W, et al. A novel tree shrew (Tupaia belangeri) model of glaucoma. *Invest Ophthalmol Vis Sci*. 2018;59:3136–3143.
6. Gao Y, Wu D, Liu D, et al. Novel acute retinal artery ischemia and reperfusion model in nonhuman primates. *Stroke*. 2020;51:2568–2572.
7. Choi M, Kim SW, Vu TQA, et al. Analysis of microvasculature in nonhuman primate macula with acute elevated intraocular pressure using optical coherence tomography angiography. *Invest Ophthalmol Vis Sci*. 2021;62(15):18.
8. Pasquale LR, Gong L, Wiggs JL, et al. Development of primary open angle glaucoma-like features in a rhesus macaque colony from southern China. *Transl Vis Sci Technol*. 2021;10(9):20.
9. McCulloch DL, Marmor MF, Brigell MG, et al. ISCEV Standard for full-field clinical electroretinography (2015 update). *Doc Ophthalmol*. 2015;130:1–12.
10. Baba H, Nakahira K, Morita N, Tanaka F, Akita H, Ikenaka K. GFAP gene expression during development of astrocyte. *Dev Neurosci*. 1997;19:49–57.
11. Xiang M, Zhou L, Macke JP, et al. The Brn-3 family of POU-domain factors: primary structure, binding specificity, and expression in subsets of retinal ganglion cells and somatosensory neurons. *J Neurosci*. 1995;15(7 Pt 1):4762–4785.

12. Cheung CMG, Teo KYC, Tun SBB, Busoy JM, Veluchamy AB, Spaide RF. Differential reperfusion patterns in retinal vascular plexuses following increase in intraocular pressure an OCT angiography study. *Sci Rep*. 2020;10(1):16505.
13. Kim BJ, Braun TA, Wordinger RJ, Clark AF. Progressive morphological changes and impaired retinal function associated with temporal regulation of gene expression after retinal ischemia/reperfusion injury in mice. *Mol Neurodegener*. 2013;8:21.
14. Johnson MA, Miller NR, Nolan T, Bernstein SL. Peripapillary Retinal Nerve Fiber Layer Swelling Predicts Peripapillary Atrophy in a Primate Model of Nonarteritic Anterior Ischemic Optic Neuropathy. *Invest Ophthalmol Vis Sci*. 2016;57(2):527–532.
15. Mergenthaler P, Dirnagl U, Meisel A. Pathophysiology of stroke: lessons from animal models. *Metab Brain Dis*. 2004;19(3-4):151–167.
16. Patel DJ, Knight CJ, Holdright DR, et al. Pathophysiology of transient myocardial ischemia in acute coronary syndromes. Characterization by continuous ST-segment monitoring. *Circulation*. 1997;95:1185–1192.
17. Osborne NN, Casson RJ, Wood JP, Chidlow G, Graham M, Melena J. Retinal ischemia: mechanisms of damage and potential therapeutic strategies. *Prog Retin Eye Res*. 2004;23:91–147.
18. Bresnick GH, Engerman R, Davis MD, de Venecia G, Myers FL. Patterns of ischemia in diabetic retinopathy. *Trans Sect Ophthalmol Am Acad Ophthalmol Otolaryngol*. 1976;81(4 Pt 1):OP694–OP709.
19. Flammer J, Mozaffarieh M. What is the present pathogenetic concept of glaucomatous optic neuropathy?. *Surv Ophthalmol*. 2007;52(Suppl. 2):S162–S173.
20. Zheng L, Gong B, Hatala DA, Kern TS. Retinal ischemia and reperfusion causes capillary degeneration: similarities to diabetes. *Invest Ophthalmol Vis Sci*. 2007;48:361–367.
21. Schmid H, Renner M, Dick HB, Joachim SC. Loss of inner retinal neurons after retinal ischemia in rats. *Invest Ophthalmol Vis Sci*. 2014;55(4):2777–2787.
22. Palmhof M, Frank V, Rappard P, et al. From Ganglion Cell to Photoreceptor Layer: timeline of deterioration in a rat ischemia/reperfusion model. *Front Cell Neurosci*. 2019;13:174.
23. Turgut B, Caliş Karanfil F. Experimental animal models for retinal and choroidal diseases. *Adv Ophthalmol Vis Syst*. 2017;7:00232.
24. Burgoyne CF. The non-human primate experimental glaucoma model. *Exp Eye Res*. 2015;141:57–73.
25. Fortune B, Yang H, Strouthidis NG, et al. The effect of acute intraocular pressure elevation on peripapillary retinal thickness, retinal nerve fiber layer thickness, and retardance. *Invest Ophthalmol Vis Sci*. 2009;50:4719–4726.
26. Ochakovski GA, Wenzel DA, Spitzer MS, et al. Retinal oedema in central retinal artery occlusion develops as a function of time. *Acta Ophthalmol*. 2020;98(6):e680–e684.
27. Cook AM, Morgan Jones G, Hawryluk GWJ, et al. Guidelines for the acute treatment of cerebral edema in neurocritical care patients. *Neurocrit Care*. 2020;32:647–666.
28. Brodtmann A, Khlif MS, Egorova N, Veldsman M, Bird LJ, Werden E. Dynamic regional brain atrophy rates in the first year after ischemic stroke. *Stroke*. 2020;51(9):e183–e192.
29. Yip LW, Yong VK, Hoh ST, Wong HT. Optical coherence tomography of optic disc swelling in acute primary angle-closure glaucoma. *Arch Ophthalmol*. 2005;123:567–569.
30. Wang L, Li C, Guo H, Kern TS, Huang K, Zheng L. Curcumin inhibits neuronal and vascular degeneration in retina after ischemia and reperfusion injury. *PLoS One*. 2011;6(8):e23194.
31. Hayreh SS, Zimmerman MB, Kimura A, Sanon A. Central retinal artery occlusion. Retinal survival time. *Exp Eye Res*. 2004;78:723–736.
32. Dijk F, Kraal-Muller E, Kamphuis W. Ischemia-induced changes of AMPA-type glutamate receptor subunit expression pattern in the rat retina: a real-time quantitative PCR study. *Invest Ophthalmol Vis Sci*. 2004;45:330–341.
33. Lee JH, Shin JM, Shin YJ, Chun MH, Oh SJ. Immunochemical changes of calbindin, calretinin and SMI32 in ischemic retinas induced by increase of intraocular pressure and by middle cerebral artery occlusion. *Anat Cell Biol*. 2011;44(1):25–34.
34. Li SY, Yang D, Yeung CM, et al. Lycium barbarum polysaccharides reduce neuronal damage, blood-retinal barrier disruption and oxidative stress in retinal ischemia/reperfusion injury. *PLoS One*. 2011;6(1):e16380.
35. Eltzschig HK, Collard CD. Vascular ischaemia and reperfusion injury. *Br Med Bull*. 2004;70:71–86.
36. Kaur C, Sivakumar V, Yong Z, Lu J, Foulds WS, Ling EA. Blood-retinal barrier disruption and ultrastructural changes in the hypoxic retina in adult rats: the beneficial effect of melatonin administration. *J Pathol*. 2007;212:429–439.
37. Sobol EK, Sakai Y, Wheelwright D, et al. Intra-arterial tissue plasminogen activator for central retinal artery occlusion. *Clin Ophthalmol*. 2021;15:601–608.